Testing the contribution of fibrinogen like 1 to the pathogenesis of metabolic dysfunction associated steatotic liver disease and hepatocellular carcinoma

Jean Personnaz[1], Lisa Cannizzo[1], Céline Marie Pauline Martin[2], Aurore Desquesnes[1], Manon Sotin[1], Joanna DaSilva[1], Hervé Guillou[2] and Léon Kautz[1].

Affiliations

[1]IRSD, Université de Toulouse, INSERM, INRAE, ENVT, Univ Toulouse III - Paul Sabatier (UPS), Toulouse, France

[2]Toxalim (Research Center in Food Toxicology), INRAE, ENVT, INP- PURPAN, UMR 1331, UPS, Université de Toulouse, Toulouse, France.

Correspondence: leon.kautz@inserm.fr or jean.personnaz@inserm.fr

Abstract

Metabolic dysfunction associated steatotic liver disease (MASLD) initiates from a simple steatosis that can evolve into hepatocellular carcinoma (HCC). The pathogensis of MASLD alters the secretion of hepatokines such as fibrinogen-like 1 (FGL1), a candidate mediator of liver steatosis and hyperglycemia. To investigate the contribution of FGL1 to liver diseases, we compared wild-type mice to mice with hepatocyte specific deletion of *Fgl1* subjected to a steatosis or HCC experimental protocol. We found that mice deficient for *Fgl1* in hepatocytes showed a reduced tolerance to glucose with pronounced metabolic alterations and liver injury when fed a western diet compared to their wild-type counterparts. However, both genotypes exhibited a similar lipid deposition in the liver. Similarly, wild type and *Fgl1* deficient mice displayed comparable liver alterations during HCC progression. We observed that *FGL1* expression was repressed during MASLD progression in mice and human concomitantly with the severity of liver injury. Altogether, these findings suggest that FGL1 is not a major contributor to the pathogenesis of MASLD and HCC.

Introduction

Metabolic dysfunction associated steatotic liver disease (MASLD), previously known as non-alcoholic fatty liver disease (NAFLD) [1] initiates from an asymptomatic steatosis affecting 30% of the worldwide population [2]. Approximately 15% of steatotic patients develop a metabolic dysfunction associated steatohepatitis (MASH, previously known as NASH), defined by the installation of fibro-inflammatory phenomenons, hepatocytes ballooning and steatosis. The MASH stage is a tipping point towards life threatening complications as 24% of MASH patients progress to a cirrhosis within 8 years and 3% of MASH patients are diagnosed with

hepatocellular carcinoma (HCC) every year [3]. MASLD currently represents the fastest growing cause of HCC worldwide [4] and a significant economic burden [2]. MASLD is the hepatic manifestation of the metabolic syndrome characterized by obesity, insulin resistance, hypertension, increased lipolysis and dyslipidemia [5] [6]. Excess of lipolysis-derived circulating fatty acids are then stored as triglycerides in the liver thereby causing steatosis [6,7]. Fat accumulation in hepatocytes triggers transcriptional modifications and secretion of hepatokines with various metabolic effects in fatty livers [8]. Among those, previous studies suggested that the induction of Fibrinogen-like 1 (FGL1) during MASLD contributed to disease progression, insulin resistance and hyperglycemia [9–11].

FGL1 is a 34kDa protein secreted by hepatocytes [12] that shares a structural homology with fibrinogen β and γ chains. FGL1 is not involved in the clotting process as it lacks the platelet binding domain, the cross linking region and the thrombin sensitive site [13]. In mice, the manipulation of FGL1 has yielded contradictory results. Administration of FGL1 after the induction of hepatic injury by 3 weeks of methionine and chlorine deficient diet reduced hepatic triglycerides content and fibrosis [14]. Conversely, mice fed and standard chow and treated with recombinant FGL1 were less sensitive to insulin [9]. *Fgl1* silencing using RNA interference was protective against high fat diet induced liver injury [10] whereas the overexpression of *Fgl1* was sufficient to induce hepatic steatosis. However, *Fgl1* deficient mice fed a standard rodent chow displayed an increased body weight, a fasting hyperglycemia and moderately reduced glucose tolerance without any modification of food intake [14,15] compared to wild type mice suggesting that FGL1 could be involved in the onset of obesity. Moreover, *Fgl1*-/- mice developed a more severe hepatocellular carcinoma induced by diethynitrosamine (DEN) [16]. Interestingly, *FGL1* gene is located on chromosome 8 both in human and mouse in a region containing several tumor suppressor genes such as *VPS37A* or *DLC1* [17]. FGL1 has also been described as a mediator of immune evasion in certain cancers [18] but this function has been questioned [19,20]. Overall, the contribution of FGL1 in the progression of MASLD remains elusive. Here, we compared the MASLD and HCC phenotype of WT mice ($FGL1^{LWT}$) and mice with hepatocyte-restricted deletion of *Fgl1* ($Fgl1^{LKO}$). We observed that $Fgl1^{LKO}$ showed increased circulating levels of liver transaminases and a trend toward a higher number of solid tumors compared to $FGL1^{LWT}$ mice. However, we did not observe any difference in steatosis and fibrosis and, in contrast with published studies, we found that FGL1 levels were decreased in mice and humans during disease progression.

Material and Methods:

Animals

Fgl1 liver knock out mice – Fgl1$^{tm1b(EUCOMM)Hmgu}$ mice were obtained from the international mouse phenotyping consortium [21] and crossed with mice expressing the FLPO recombinase (C57BL/6-Tg(CAG-Flpo)1Afst/Ieg; MMRRC_036512-UCD) to remove the EUCOMM cassette flanked by FRT site resulting in *Fgl1* floxed (*Fgl1$^{fl/fl}$)* mice. *Fgl1$^{fl/fl}$* mice were then bred with mice expressing the CRE recombinase under the control of the albumin promoter (B6.Cg-Speer6-$^{ps1Tg(Alb-cre)21Mgn/J}$, Jackson laboratory stain #003574) to obtain mice with hepatocytes specific ablation of *Fgl1 (Fg1^{LKO}*) or wild type *Fgl1$^{fl/fl}$* littermate mice *(Fgl^{LWT}*) [22]. Mice were bred and housed at Janvier Laboratories (Le Genest St Isle, France) and transferred to the CREFRE US006 animal care facility at 4 to 5 weeks of age. 6 week-old C57BL/6J were purchased from Envigo. Mice were housed in a specific and opportunistic pathogen-free facility under a 12-hour light -dark cycle with *ad libitum* access to water and standard laboratory mouse chow diet (SAFE A04), in accordance with the European Union guidelines, and then subjected to a dietary challenge between 6 to 8 weeks of age. The study was performed in compliance with the European guidelines for the use and care of laboratory animals, and approved by an independent ethics committee (CEEA 122) under the authorization numbers APAFIS #40791-202302021502788.

Western diet model – *Fgl1^{LWT}* and *Fgl1^{LKO}* mice were fed a standard rodent chow (SAFE A04) or a western diet containing 35% sucrose, 20% lipids et 0,15% cholesterol (Research diet D12079B) for 16 weeks with free access to water.

Oral glucose tolerance test – Mice were housed in clean cages without food for 16h. Baseline glycemia was first measured using a glucometer (FreeStyle Optium Neo, Abbott) and a drop blood harvested at the tail vein. 30 minutes later, mice were administered a 1.5g/kg bolus of a D-Glucose solution *per os.* Glycemia was recorded over 120 minutes.

HCC model – *Fgl1^{LWT}* and *Fgl1^{LKO}* mice were fed a western diet containing 35% sucrose, 20% lipids et 0,15% cholesterol (Research diet D12079B) with weekly intraperitoneal injection of carbon tetrachloride (CCl_4, 0.2µl/g) [23] for 24 weeks.

Genotyping

After digestion with 25mM NaOH, 0.2M EDTA and neutralization with 40mM Tris-HCl, PCRs were performed using the following primers: Alb-CRE (FW1: TGCAAACATCACATGCACAC, FW2: GAAGCAGAAGCTTAGGAAGATGG , RV: TTGGCCCCTTACCATAACTG LoxpP sites (FW: TGTGCAGACTGTCATCTCAGTACAGCC, RV: TGTGCAGACTGTCATCTCAGTACAGCC. The excision of *FGL1* exon 2 in the liver was

confirmed using the following primers: FW: TGTGCAGACTGTCATCTCAGTACAGCC, RV: GGCAGAGCTCGAGCATTAGCAGA.

Biochemical analysis

Whole blood was collected with K_3-EDTA (Sigma) to prevent clotting and the plasma was prepared by two successive centrifugations (3000rpm at 4°C for 5min). Levels of triglycerides, cholesterol, alanine and aspartate aminotransferases were determined by the Anexplo Phenotyping facility using a Pentra400 biochemical analyzer (HORIBA Medical, Kyoto, Japan).

Neutral lipids analysis

Lipids from 1mg of liver weight were extracted using adapted Bligh and Dyer method [24] in dichloromethane/methanol (2% acetic acid) /water (2.5:2.5:2 v/v/v), stigmasterol, cholesteryl heptadecanoate and glyceryl trinonadecanoate were used as internal standards. The solution was centrifuged at 2500 rpm for 6 min. The organic phase was collected and dried under nitrogen, then dissolved in 20 µL of ethyl acetate. 1µl of the lipid extract was analyzed by liquid-gas chromatography on a Trace 1600 (Thermo Electron) system using a RTX-5 Restek fused silica capillary column (5mx0.25mm ID, 0.50 µm film thickness) [25]. The oven temperature was programmed from 200°C to 350°C at a rate of 5°C per minute, and the carrier gas used was hydrogen (0.5 bar). The injector and detector temperatures were set at 315°C and 345°C, respectively.

RNA extraction, RT and qPCR

Total RNA from mouse tissues was extracted by Trizol (MRC) / Chloroform (Sigma) method. Complementary cDNA was synthetized using M-MLV Reverse transcriptase (Promega). Messenger RNA (mRNA) expression levels were assessed by quantitative polymerase chain reaction (RT-qPCR) using Takyon SYBR green (Eurogentec) (primers indicated in supplemental table 1) and run on a LightCycler480 (Roche) apparatus. Transcript abundance was normalized to the reference gene *Rpl4* and represented as a difference between reference and target genes within each group of mice (−ΔCt) ± standard error of the mean (SEM).

Histology

Liver biopsies were fixed in 4% formaldehyde for 24 hours before paraffin-embedding. 5 µm sections of paraffin-embedded livers were stained with hematoxylin and eosin (H&E, Sigma) or with picrosirius red (Sirius red, Abcam) according to standard protocols. A NAFLD activity score (NAS) [26] was computed.

Statistical analysis

All data are expressed as mean ± standard error of the mean (SEM). Statistical significance was assessed by Student t test, 1- or 2-way analysis of variance followed by post-hoc test as specified in the figure legends using GraphPad Prism version 10. P values <0.05 were considered significant (*P < 0.05; **P < 0.01; ***P < 0.001; ****P < 0.0001).

Results

Hepatocyte specific deletion *Fgl1* promotes body weight gain and glucose intolerance. *Fgl1* floxed mice were bred with mice expressing the CRE recombinase under the albumin promoter to invalidate Fgl1 specifically in hepatocytes. Excision of *FGL1* exon 2 (Figure 1A) led to a significant reduction in whole liver *Fgl1* mRNA expression (Figure 1B). *Fgl1* liver-knockout mice ($Fgl1^{LKO}$) displayed increased body weight compared to wild type littermate ($Fgl1^{LWT}$, Figure 1C) but no difference in liver (Figure 1D) and epididymal (eWAT, Figure 1E) relative weight was observed. In contrast, inguinal fat (iWAT) deposit weight relative to total body weight was significantly increased in $Fgl1^{LKO}$ mice (Figure 1F) compared $Fgl1^{LWT}$ animals, presumably explaining the increase in body weight. $Fgl1^{LKO}$ mice also exhibited an increased glycemia after overnight fasting and during an oral glucose tolerance test (oGTT, Figure 1G and 1H) indicating a reduced oral glucose tolerance. Collectively, these results indicate that *Fgl1* deletion specifically in hepatocytes in sufficient to recapitulate the previously reported phenotype of mice with whole-body ablation of *Fgl1* [15,27].

Deletion of hepatocyte *Fgl1* promotes metabolic alterations incuded by western diet. Previous studies suggested that FGL1 could be involved in the pathogenesis of MASLD [9,10,14,15,28] but whether this contribution is protective or detrimental is unclear. In order to investigate the contribution of hepatocyte FGL1 in MASLD, $Fgl1^{LWT}$ and $Fgl1^{LKO}$ mice were fed a western diet for 16 weeks (WD). Western diet-fed mice develop obesity coupled with moderate intolerance to glucose, hepatic steatosis and inflammation [29]. Both genotypes gained a comparable weight when fed either the standard (Figure 2A) or the western diet (Figure 2B). After 16 weeks, $Fgl1^{LWT}$ and $Fgl1^{LKO}$ fed a standard diet showed a comparable glycemia and glucose tolerance (Figure 2C) whereas $Fgl1^{LKO}$ mice fed a western diet presented with higher glucose levels after fasting and glucose tolerance test as shown by the increased A.U.C. (Figure 2D) compared to their WT counterparts. Liver (Figure 2E) and iWAT (Figure2F) relative weights were significantly increased only in $Fgl1^{LKO}$ fed a WD in comparison to mice on normal chow whereas the eWAT relative weight was significantly decreased in $Fgl1^{LWT}$ (Figure 2G). Circulating triglycerides were unchanged but $Fgl1^{LWT}$ and $Fgl1^{LKO}$ mice fed a WD showed a significant increase in circulating cholesterol compared to mice fed a normal chow (Figure 2H-I). Similarly, circulating levels of alanine (ALT) and aspartate aminotransferases (AST) (Figure

2J-K) were increased in mice fed a western diet compared to mice fed a normal chow. When fed a WD, *Fgl1*^{LKO} mice had higher levels of circulating transaminases compared to *Fgl1*^{LWT} suggesting a more severe liver injury. We next analyzed liver tissue sections stained with hematoxylin and eosin (H&E) or sirius-red to assess the extent of liver damage. We observed that both *Fgl1*^{LWT} and *Fgl1*^{LKO} mice developed a comparable microvesicular steatosis in comparison to mice fed a normal chow (Figure 3A) whereas no sign of fibrosis was observed (Figure 3B). While the steatosis was comparable between *Fgl1*^{LWT} and *Fgl1*^{LKO} fed a western diet, a significant increase was observed only in *Fgl1*^{LKO} when compared to mice fed a normal chow (Figure 3C). We observed a significant and comparable increase in hepatic triglycerides and cholesterol levels (Figure 3D-E). Consistent with a comparable steatosis, a mild albeit significant induction in lipogenesis marker *Scd1* and the inflammation and steatosis marker *Fasn* mRNA expression was observed in mice fed a western diet compared to mice fed a normal chow (Figure 3F). Consistent with the sirius-red staining, hepatic mRNA expression of *Col1a1* encoding the pro-α1 chain of procollagen or *Acta2* encoding the smooth-muscle actin was similar between animals fed a standard or a western diet (Figure 3G). mRNA expression of the inflammatory markers *Cd45* and *Emr1* (also known as F4/80, Figure 3H) was significantly increased in mice fed a WD but no difference was observed between *Fgl1*^{LWT} and *Fgl1*^{LKO}. Altogether, these results suggest that the deletion of *Fgl1* sensitizes mice to diet-induced glucose intolerance but that it only has a limited effect on MASH-related liver injury at this time point.

FGL1 deletion does not influence the progression of hepatocellular carcinoma. To assess the effect of *Fgl1* deletion in the onset and progression of HCC, we applied a protocol combining a western diet with weekly injection of CCl_4 for 24 weeks [23]. In this model both genotypes exhibited limited weight gain when fed a western diet (Figure 4A). After 24 weeks, both genotypes displayed similar liver to body weight ratio (Figure 4B) and circulating levels of ALT and AST (Figure 4C-D). However, we observed that 30% of *Fgl1*^{LKO} mice presented with macroscopic liver tumors (Figure 4E), suggesting an increased susceptibility of *Fgl1*^{LKO} to carcinogenesis, as previously described [16]. We next assessed the extend of liver damages and liver fibrosis on histological sections stained with hematoxyline and eosin or sirius red sain and a NAS score was computed (Figure 4F-G). No difference was observed between *Fgl1*^{WT} and *Fgl1*^{LKO}, suggesting similar liver damages. mRNA levels of markers of inflammation (*Il6* and *Il1-b*) or fibrosis (*Acta2* and *Col1a1)* Figure 4H) and immune cells infiltration (*Cd45, Ly6g, Cd3e* and *Emr1*, Figure 4I) were similar between both genotypes. We found that *Emr1* expression was increased in *Fgl1*^{LKO} but the protein level was comparable when liver tissue section were stained for F4/80 (Figure 4J). Together our data suggest that the deletion of FGL1 has limited effect on HCC installation and progression.

***Fgl1* expression is repressed during the progression of MASLD in mice and human–** In Contrast to previous studies[9,10], we found that liver *Fgl1* mRNA expression was significantly reduced in mice subjected to a MASH or a HCC protocol in comparison to mice fed a standard diet for 8 weeks (Figure 5A). Retrospective analysis of published datasets from studies of MASH or HCC patients (GSE48452[30], GSE164760[31] and GSE14520[32]) revealed that *FGL1* expression was significantly reduced in patients suffering from MASH and HCC (Figure 5B-D). We therefore decided to study the time-course of *Fgl1* mRNA expression in the liver of mice fed a western diet for 8 weeks. We observed a gradual increase in steatosis and NAS score (Figure 5E-F) over 8 weeks but at this time-point circulating levels of ALT and AST were unchanged (Figure 5G). *Fgl1* mRNA expression was first induced after 4 weeks on western diet but decreased significantly 4 to 8 weeks after the mice were placed on western diet (Figure 5H). Interestingly, while the expression of the inflammatory marker *Socs3* and was unchanged (Figure 5I), *Fgl1* expression was inversely correlated with the expression of markers of ER stress (*Ddit3*) and immune cells infiltration (*Cd45*) (Figure 5J-K). The results confirm that *Fgl1* expression is repressed during the early phases of MASLD.

Discussion

Over the past decade, hepatokines have emerged as potential contributors of the pathogenesis of MASLD [8], a complex pathology associated with multi-organ metabolic dysfunctions. Among those, the importance of FGL1 in the progression of MASLD remains largely speculative. While its official symbol is FGL1 for Fibrinogen-like 1, it is also commonly referred to as hepassocin (HPS) or HFREP1 in studies that have yielded sometimes opposite conclusions depending on the strategy used to assess the potential function of FGL1 in metabolic diseases. These include transient knock-downs using shRNA, lentiviral-based overexpression, recombinant protein administration in combination with diet or genetically (*i.e.* Ob/Ob mice) induced metabolic dysfunctions. Since FGL1 is secreted predominantly by hepatocytes, we examined for the first time whether hepatocyte-derived FGL1 is involved in the progression of MASLD using mice with ablation of *Fgl1* specifically in hepatocytes fed a western diet for 16 weeks, a model that recapitulates the features of the pathology described in human [23]. We found that *Fgl1*^{LKO} mice exhibited slightly increased liver damages, as shown by elevated AST, ALT and triglyceride levels suggesting an increased sensitivity to diet-induced liver injury. However, we did not detect any difference in lipid accumulation in the liver and the MASH phenotype was comparable to their WT controls. In mice, administration of recombinant FGL1 or its overexpression using a lentiviral vector was previously shown to induce insulin resistance through the ERK1/2 signaling pathway whereas its lentiviral knockdown improved insulin resistance in mice fed a high fat diet or genetically obese Ob/Ob

mice [9]. The same group also used lentiviral vectors or short-hairpin RNA to show that, in mice fed a high fat diet for 12 weeks, overexpression of FGL1 increased hepatic lipid accumulation and NAFLD score whereas its knockdown reduced the steatosis and the NAS score [10]. We observed a comparable increase in circulating transminases levels in mice fed a western diet for 16 weeks compared to mice fed a normal chow. However, we reached opposite conclusions as our results indicate that genetic deletion of FGL1 in hepatocytes was accompanied by an increase in ALT, AST and triglycerides levels compared to WT mice. Our results are in line with a recent study showing that whole-body *Fgl1* knock out developed a more pronounced steatosis than their WT counterparts when fed a high fat for 16 weeks or a methionine-choline deficient (MCD) diet for 3 weeks [14]. Daily injections of recombinant FGL1 (1mg/kg) for a week was sufficient to ameliorate the steatosis and insulin resistance in mice fed a HFD (16 weeks) or MCD (3 weeks) diet [14]. Similarly, *Fgl1* silencing using siRNA enhanced liver injury induced by D-galactosamine in mice [33] whereas the administration of recombinant FGL1 to Cynomolgus monkeys limited the extent of liver injury induced by D-Galactosamine administration [34]. Of note, we tested the antibobies used to assess liver FGL1 protein levels in mouse [9,10,14] and observed a similar protein profile in liver extracts from WT or *Fgl1-/-* mice (data not shown) indicating that the antibodies to mouse FGL1 are largely unspecific.

Importantly, we found that *Fgl1* expression was significantly increased after 4 weeks on western diet (*i.e.* during the onset of the steatosis) and subsequently reduced after 6-16 weeks when the steatosis progressed. Two additional study described a similar bi-phasic regulation of *Fgl1* transcription during liver diseases. In mice fed a MCD diet, liver *Fgl1* mRNA expression was increased after a week and progressively decreased over 2-6 weeks of dietary challenge [14]. A similar downregulation of *Fgl1* mRNA expression was observed in MASH patients and in the liver of 4-12 weeks-old *Ob/Ob* mice. FGL1 protein levels were presumably increased when mice were fed a high fat diet containing 45% lipids and significantly reduced after 24-40 weeks [14]. An increase in FGL1 expression or protein levels was also observed in the liver of mice fed a high fat diet for 12 weeks [9,10] but, while we questioned the reliability of the antibodies, the mRNA expression data were not provided for these sets of mice. The transcription of *Fgl1* is regulated by inflammatory cytokines such as Interleukin-6 in cooperation with the hepatocyte nuclear factor 1α (HNF1α) [14,35] and the high-mobility group box 1 protein (HMGB1) which could explain the induction of *Fgl1* during the early phases [36] but we did not notice any change in the expression of the inflammatory marker *Socs3*. Similarly, *Fgl1* tanscription is stimulated during ER stress [27] but we did not observe any change in mRNA expression of target genes *Ddit3* (ER stress) and the mechanism regulating *Fgl1* expression during metabolic alterations is still unknown. The present work support the most

recent studies [14,37,38] suggesting that FGL1 may exert a protective function during the progression of steatosis but its exact function is still unknown.

Interestingly, 8 weeks old *Fgl1*^{LKO} mice fed a normal chow displayed an increased adiposity compared to their WT controls. A similar phenotype was observed in *Fgl1-/-* mice by Demchev and colleagues [15]. However, the same group that used lentivriral vectors to assess the contribution of FGL1 in MASLD described that lentiviral overexpression of *Fgl1* in epididymal fat pads increased the fat pads whereas its inhibition decreased the high fat diet induced adiposity [28]. This further emphasizes the discrepancies between the genetic and lentiviral manipulation of FGL1 suggesting that the absence of FGL1 during development and at birth could predispose to a different response during metabolic cues in comparions to a transient inactivation. As the expression of *Fgl1* in adipose tissue is very low [39], the phenotype could also be attributable to lentiviral vectors off-target effects. The molecular mechanisms involved in the inter-organ dialogue between hepatocyte-derived FGL1 and the adipose tissue therefore remain uncertain.

FGL1 has also been described as a mediator of immune evasion in certain cancers such as non-small cells lung cancer or metastatic melanoma [18]. The binding of FGL1 to its receptor lymphocytes activating gene 3 (LAG3) [18] at the cell surface of activated T lymphocytes promotes T cells exhaustion and inactivation and prevents their anti-tumoral activity [18]. While we observed a trend toward more solid tumors in *Fgl1*^{LKO} mice compared to *Fgl1*^{LWT} mice, both genotypes exhibited a similar HCC phenotype with the exception of a higher expression of *Emr1* mRNA in the liver of *Fgl1*^{LKO} mice that was not found when comparing protein abundance. As the expression of LAG3 is low in the liver [40], the FGL1/LAG3 interaction may not contribute to liver cancer. Moreover, this mechanism has been recently questioned [19,20] and FGL1 may only have a weak tumorigenic activity.

FGL1 has been originally described as an hepatocytes mitogen [12,33,41,42]. Although knockdown of FGL1 during zebrafish embryogenesis using morpholino reduced the proliferation of hepatocytes and the size of the liver, such phenotype was not observed in *Fgl1-/-* mice. In Human, the downregulation of FGL1 is found in 20% [18] to 60% [38] of liver cancer and its expression correlated with the degree of tumor differentiation. FGL1 is located on chromosome 8p, a region where cumulative allelic loss have been positively correlated with aggressive tumors [17,43]. Conversely, high *FGL1* expression was significantly associated with larger tumor size and liver cirrhosis [44]. The study of FGL1 protein level in human will await the development of new analytical tools and standardized methods. Indeed, published results of FGL1 measurement using commercial ELISAs should be interpreted with caution as the

baseline levels in healthy patients ranged from 690 pg/mL to 6 mg/µL. Whether the downregulation of *Fgl1* contributes to the pathogenesis of MASLD and HCC will therefore require further investigation.

Acknowledgments:

The authors thank Céline Deraison (Inserm U1220) and Nicolas Blanchard (Inserm U1291) for providing the FLP1 mice, members of the INSERM US006 animal, histopathology and phenotyping facility facilities (Toulouse) and the platform Aninfimip, an EquipEx ('Equipement d'Excellence') supported by the French government through the Investments for the Future program, Nancy Geoffre and Justin Bertrand-Michel from MetaToul (Toulouse metabolomics & fluxomics facilities, www.metatoul.fr) which is part of the French National Infrastructure for Metabolomics and Fluxomics MetaboHUB-ANR-11-INBS-0010 (doi.org/10.15454/VRJK-KY76). Support for this work was provided by the French National Research Agency (ANR-16-ACHN-0002-01 and ANR-22-CE14-0076-01), the region Occitanie and by the European Research Council (ERC) under the European Union's Horizon 2020 research and innovation program (grant agreement no. 715491) to LK and by ARC (ARCPOST-DOC2022020004813) and FRM (ARF202209015711) postdoctoral fellowship to JP.

Authorship Contributions: JP, LC, CMPM, AD, MS, JDS performed experiments and analyzed data. JP, HG and LK designed and supervised the study, analyzed data and wrote the manuscript. All authors edited the manuscript.

References :

1. Rinella, M. E. & Sookoian, S. From NAFLD to MASLD: updated naming and diagnosis criteria for fatty liver disease. *Journal of Lipid Research* **65**, 100485 (2024).
2. Younossi, Z. M. *et al.* The economic and clinical burden of nonalcoholic fatty liver disease in the United States and Europe. *Hepatology* **64**, 1577–1586 (2016).
3. Toh, M. R. *et al.* Global Epidemiology and Genetics of Hepatocellular Carcinoma. *Gastroenterology* **164**, 766–782 (2023).
4. Huang, D. Q., El-Serag, H. B. & Loomba, R. Global epidemiology of NAFLD-related HCC: trends, predictions, risk factors and prevention. *Nat Rev Gastroenterol Hepatol* **18**, 223–238 (2021).
5. Roberts, C. K., Hevener, A. L. & Barnard, R. J. Metabolic Syndrome and Insulin Resistance: Underlying Causes and Modification by Exercise Training. in *Comprehensive Physiology* (ed. Prakash, Y. S.) 1–58 (Wiley, 2013). doi:10.1002/cphy.c110062.
6. Lee, E., Korf, H. & Vidal-Puig, A. An adipocentric perspective on the development and progression of non-alcoholic fatty liver disease. *Journal of Hepatology* **78**, 1048–1062 (2023).
7. Donnelly, K. L. *et al.* Sources of fatty acids stored in liver and secreted via lipoproteins in patients with nonalcoholic fatty liver disease. the (2005) doi:10.1172/JCI23621.
8. Stefan, N., Schick, F., Birkenfeld, A. L., Häring, H.-U. & White, M. F. The role of hepatokines in NAFLD. *Cell Metabolism* **35**, 236–252 (2023).
9. Wu, H.-T. *et al.* A novel hepatokine, HFREP1, plays a crucial role in the development of insulin resistance and type 2 diabetes. *Diabetologia* **59**, 1732–1742 (2016).
10. Wu, H.-T. *et al.* The role of Hepassocin in the development of non-alcoholic fatty liver disease. *Journal of Hepatology* **59**, 1065–1072 (2013).
11. Jung, T. W., Chung, Y. H., Kim, H.-C., Abd El-Aty, A. M. & Jeong, J. H. Hyperlipidemia-induced hepassocin in the liver contributes to insulin resistance in skeletal muscle. *Molecular and Cellular Endocrinology* **470**, 26–33 (2018).

12. Hara, H. *et al.* Isolation and characterization of a novel liver-specific gene, hepassocin, upregulated during liver regeneration. *Biochimica et Biophysica Acta* (2000).
13. Personnaz, J., Guillou, H. & Kautz, L. Fibrinogen-like 1: A hepatokine linking liver physiology to hematology. *HemaSphere* **8**, e115 (2024).
14. Yang, Y. *et al.* HPS protects the liver against steatosis, cell death, inflammation, and fibrosis in mice with steatohepatitis. *The FEBS Journal* **289**, 5279–5304 (2022).
15. Demchev, V. *et al.* Targeted Deletion of Fibrinogen Like Protein 1 Reveals a Novel Role in Energy Substrate Utilization. *PLOS ONE* **8**, e58084 (2013).
16. Nayeb-Hashemi, H. *et al.* Targeted disruption of fibrinogen like protein-1 accelerates hepatocellular carcinoma development. *Biochemical and Biophysical Research Communications* **465**, 167–173 (2015).
17. Xue, W. *et al.* A cluster of cooperating tumor-suppressor gene candidates in chromosomal deletions. *Proc. Natl. Acad. Sci. U.S.A.* **109**, 8212–8217 (2012).
18. Wang, J. *et al.* Fibrinogen-like Protein 1 Is a Major Immune Inhibitory Ligand of LAG-3. *Cell* **176**, 334-347.e12 (2019).
19. Maruhashi, T. *et al.* Binding of LAG-3 to stable peptide-MHC class II limits T cell function and suppresses autoimmunity and anti-cancer immunity. *Immunity* **55**, 912-924.e8 (2022).
20. Ming, Q. *et al.* LAG3 ectodomain structure reveals functional interfaces for ligand and antibody recognition. *Nat Immunol* **23**, 1031–1041 (2022).
21. Groza, T. *et al.* The International Mouse Phenotyping Consortium: comprehensive knockout phenotyping underpinning the study of human disease. *Nucleic Acids Research* **51**, D1038–D1045 (2023).
22. Coleman, J. L. J. *et al.* Rapid Knockout and Reporter Mouse Line Generation and Breeding Colony Establishment Using EUCOMM Conditional-Ready Embryonic Stem Cells: A Case Study. *Front. Endocrinol.* **6**, (2015).
23. Tsuchida, T. *et al.* A simple diet- and chemical-induced murine NASH model with rapid progression of steatohepatitis, fibrosis and liver cancer. *Journal of Hepatology* **69**, 385–395 (2018).

24. Bligh, E. G. & Dyer, W. J. A rapid method of total lipid extraction and purification. *Can. J. Biochem. Physiol.* **37**, 911–917 (1959).
25. Barrans, A. *et al.* Hepatic lipase induces the formation of pre-beta 1 high density lipoprotein (HDL) from triacylglycerol-rich HDL2. A study comparing liver perfusion to in vitro incubation with lipases. *Journal of Biological Chemistry* **269**, 11572–11577 (1994).
26. Kleiner, D. E. *et al.* Design and validation of a histological scoring system for nonalcoholic fatty liver disease. *Hepatology* **41**, 1313–1321 (2005).
27. Yang, Y. *et al.* Protective Role of Hepassocin against Hepatic Endoplasmic Reticulum Stress in Mice. *IJMS* **23**, 13325 (2022).
28. Wu, H.-T. *et al.* Targeting fibrinogen-like protein 1 is a novel therapeutic strategy to combat obesity. *The FASEB Journal* **34**, 2958–2967 (2020).
29. Smati, S. *et al.* Integrative study of diet-induced mouse models of NAFLD identifies PPARα as a sexually dimorphic drug target. *Gut* **71**, 807–821 (2022).
30. Ahrens, M. *et al.* DNA Methylation Analysis in Nonalcoholic Fatty Liver Disease Suggests Distinct Disease-Specific and Remodeling Signatures after Bariatric Surgery. *Cell Metabolism* **18**, 296–302 (2013).
31. Pinyol, R. *et al.* Molecular characterisation of hepatocellular carcinoma in patients with non-alcoholic steatohepatitis. *Journal of Hepatology* **75**, 865–878 (2021).
32. Roessler, S. *et al.* A Unique Metastasis Gene Signature Enables Prediction of Tumor Relapse in Early-Stage Hepatocellular Carcinoma Patients. *Cancer Research* **70**, 10202–10212 (2010).
33. Li, C. Y. *et al.* Recombinant human hepassocin stimulates proliferation of hepatocytes in vivo and improves survival in rats with fulminant hepatic failure. *Gut* **59**, 817–826 (2010).
34. Yang, Y. *et al.* Recombinant Human HPS Protects Mice and Nonhuman Primates from Acute Liver Injury. *IJMS* **22**, 12886 (2021).
35. Yu, H.-T. *et al.* Specific Expression and Regulation of Hepassocin in the Liver and Down-regulation of the Correlation of HNF1α with Decreased Levels of Hepassocin in Human Hepatocellular Carcinoma. *Journal of Biological Chemistry* **284**, 13335–13347 (2009).

36. Liu, Z. & Ukomadu, C. Fibrinogen-like protein 1, a hepatocyte derived protein is an acute phase reactant. *Biochemical and Biophysical Research Communications* **365**, 729–734 (2008).
37. Sardo, U. *et al.* The hepatokine FGL1 regulates hepcidin and iron metabolism during anemia in mice by antagonizing BMP signaling. *Blood Journal* blood.2023022724 (2023) doi:10.1182/blood.2023022724.
38. Yan, J. *et al.* LFIRE-1/HFREP-1, a liver-specific gene, is frequently downregulated and has growth suppressor activity in hepatocellular carcinoma. *Oncogene* **23**, 1939–1949 (2004).
39. Yamamoto, T. *et al.* Molecular Cloning and Initial Characterization of a Novel Fibrinogen-Related Gene, HFREP-1. *Biochemical and Biophysical Research Communications* **193**, 681–687 (1993).
40. Huard, B., Gaulard, P., Faure, F., Hercend, T. & Triebel, F. Cellular expression and tissue distribution of the human LAG-3-encoded protein, an MHC class II ligand. *Immunogenetics* **39**, (1994).
41. Hara, H. *et al.* Molecular cloning and functional expression analysis of a cDNA for human hepassocin, a liver-specific protein with hepatocyte mitogenic activity. *Biochimica et Biophysica Acta* (2001).
42. Yan, J. *et al.* Cloning and characterization of a mouse liver-specific gene mfrep-1, upregulated in liver regeneration. *Cell Res* **12**, 353–361 (2002).
43. Chan, K.-L., Man-Fong Lee, J., Guan, X.-Y., Fan, S.-T. & Oi-Lin Ng, I. High-density allelotyping of chromosome 8p in hepatocellular carcinoma and clinicopathologic correlation. *Cancer* **94**, 3179–3185 (2002).
44. Lin, M. *et al.* Targeting fibrinogen-like protein 1 enhances immunotherapy in hepatocellular carcinoma. *Journal of Clinical Investigation* **133**, e164528 (2023).

Figure legends

Figure 1: Hepatocyte specific deletion of *Fgl1* recapitulates the phenotype of whole-body knockout mice. Validation of *Fgl1* exon 2 excision by PCR on primary hepatocytes (A). Whole liver *Fgl1* mRNA expression (B). Body weight (C) and relative liver (D), epididymal adipose tissue (eWAT, E) and inguinal adipose tissue (iWAT, F) relative weighs in WT (n=5) and LKO (n=8) males mice fed a normal chow. Fasting glycemia (G) and oral glucose tolerance test (1,5g/kg) were measured and A.U.C. was calculated (H) in males wild-type (WT, n=7) or *Fgl1* liver knockout (LKO, n=8) mice fed a normal chow. Data are mean ± SEM. Statistical significance was assayed by Student's t-test (B-H) or by 2-way ANOVA, followed by Šídák's multiple comparisons test (H). *p<0.05, **p<0.01, ***p<0.001

Figure 2: Hepatocytes deletion of FGL1 sensitizes mice to diet-induced liver injury . *Fgl1* WT ($Fgl1^{LWT}$) or *Fgl1* liver knock out ($Fgl1^{LKO}$) male mice were fed a western diet 16-weeks. Body weight gain in mice fed a normal chow (A) or a western diet (B). Oral glucose tolerance was assessed after 16 weeks (C-D). Liver (E), iWAT (F) and eWAT (G) to body weight ratios . Circulating levels of triglycerides (H), cholesterol (I), aspartate (AST) (J) and alanine (ALT) (K) aminotransferases. Data are means ± SEM (WT NC n=5, LKO NC n=6, WT WD n=8, LKO WD n=9) and were compared by 2-way ANOVA followed by Holm-Šídák's multiple comparisons test, *p<0.05, **p<0.01, ***p<0.001, ****p<0.0001.

Figure 3: $Fgl1^{LWT}$ and $Fgl1^{LKO}$ mice displayed similar liver injury. Liver tissue sections were stained with hematoxylin and eosin (A) or Sirius red (B) and the diseases activity score (NAS, C) was computed. Scale bar is 100µm. Liver cholesterol (D) and triglycerides (E) content. mRNA expression of lipogenesis (*Scd1* and *Fasn*, F), fibrosis (*Col1a1, Acta2,* G) and immune cells markers (*Cd45* and *Emr1,* H) was measured by qPCR. Data are means ± SEM (WT NC n=5, LKO NC n=6, WT WD n=8, LKO WD n=9) and were compared by two-way ANOVA followed by Holm-Šídák's multiple comparisons test, **p<0.01, ***p<0.001, ****p<0.0001.

Figure 4: FGL1 does not contribute to the progression of cirrhosis/HCC. $Fgl1^{LWT}$ (n=11) and $Fgl1^{LKO}$ (n=9) male mice were fed a western diet for 24 weeks and given weekly intra peritoneal injections of carbon tertrachloride (CCl_4, 0.2µL/g). Body weight (A), Liver to body weight ratio (B) and circulating alanine (ALT, C) and aspartate (AST, D) amino transferase levels. Percentage of observed liver macroscopic tumor (E). NAS score (F) and liver tissue sections stained with hematoxylin or picrosirius (G). Liver mRNA expression of inflammation, fibrosis (H) and immune cells infiltration (I) were measured by qPCR. Liver sections were

stained for F4/80 (J) . Data are means ± SEM. And were compared by two-way ANOVA followed by Holm-Šídák's multiple comparisons test (A) or Student's t-test (B-J), **p<0.01.

Figure 5: *Fgl1* expression is rapidly repressed during the onset of steatosis. Liver *Fgl1* expression was measured in the liver of WT mice fed a normal chow (healthy, n=8) or western diet (MASH, n=8) for 16 weeks or a western diet + CCl_4 for 24 weeks (HCC, n=10) (A). retrospective analysis of *FGL1* expression in published datasets GSE48452 (B), GSE164760 (C) and GSE14520 (D)). Liver tissue sections stained with hematoxylin (n=5 per time-point) (E), NAS score (F) and circulating levels of ALT and AST (G). Liver *Fgl1* (H)*, Socs3* (I)*, Ddit3* (J) and *Cd45* (K) mRNA expression. Data are means ± SEM were compared by . Statistical significance was assayed by Student's t-test (A-D) or one-way ANOVA followed by Holm-Šídák's multiple comparisons test (F-K), *p<0.05, **p<0.01, ***p<0.001, ****p<0.0001.

Figures

Figure 1

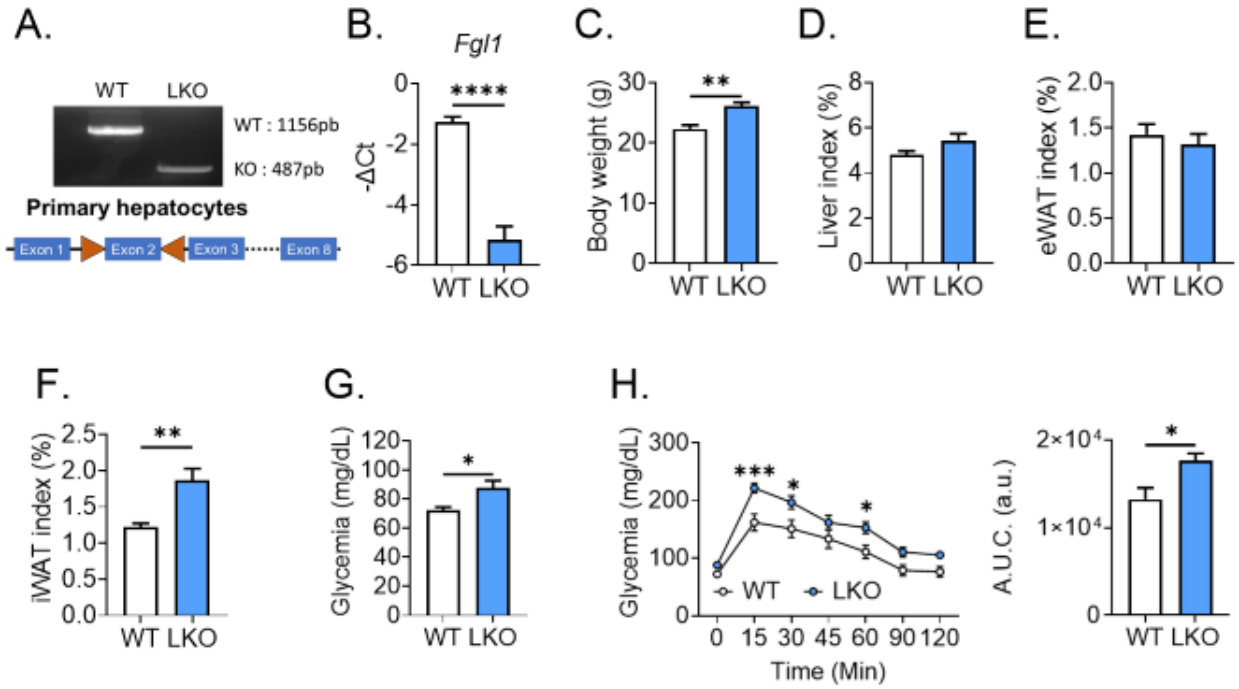

Figure 2

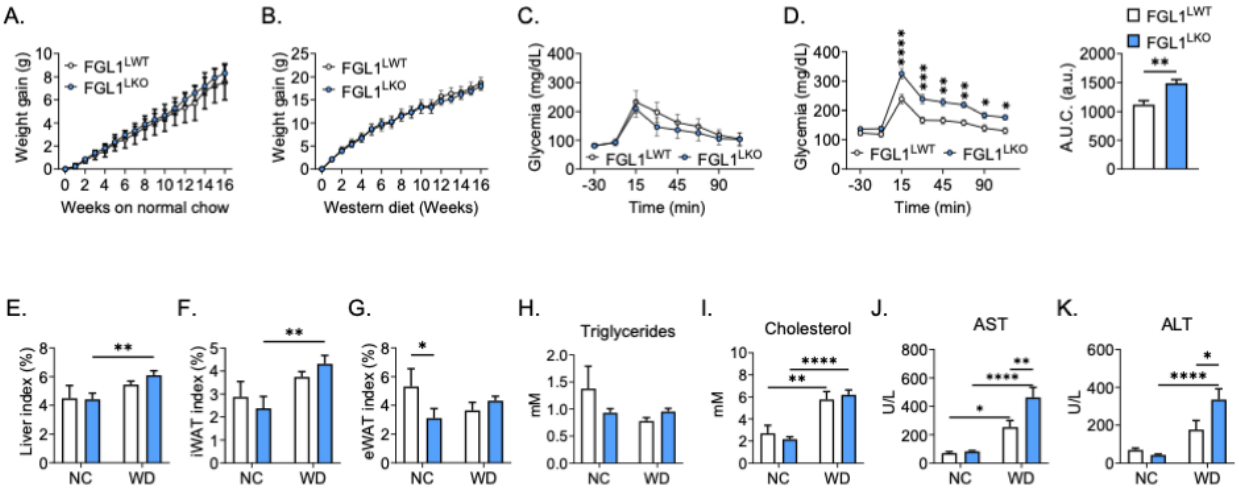
A.
Weight gain (g)
FGL1LWT
FGL1LKO
Weeks on normal chow
B.
Weight gain (g)
FGL1LWT
FGL1LKO
Western diet (Weeks)
C.
Glycemia (mg/dL)
FGL1LWT
FGL1LKO
Time (min)
D.
Glycemia (mg/dL)
FGL1LWT
FGL1LKO
Time (min)
FGL1LWT
FGL1LKO
A.U.C. (a.u.)
E.
Liver index (%)
NC
WD
F.
iWAT index (%)
NC
WD
G.
eWAT index (%)
NC
WD
H.
Triglycerides
mM
NC
WD
I.
Cholesterol
mM
NC
WD
J.
AST
U/L
NC
WD
K.
ALT
U/L
NC
WD

Figure 3

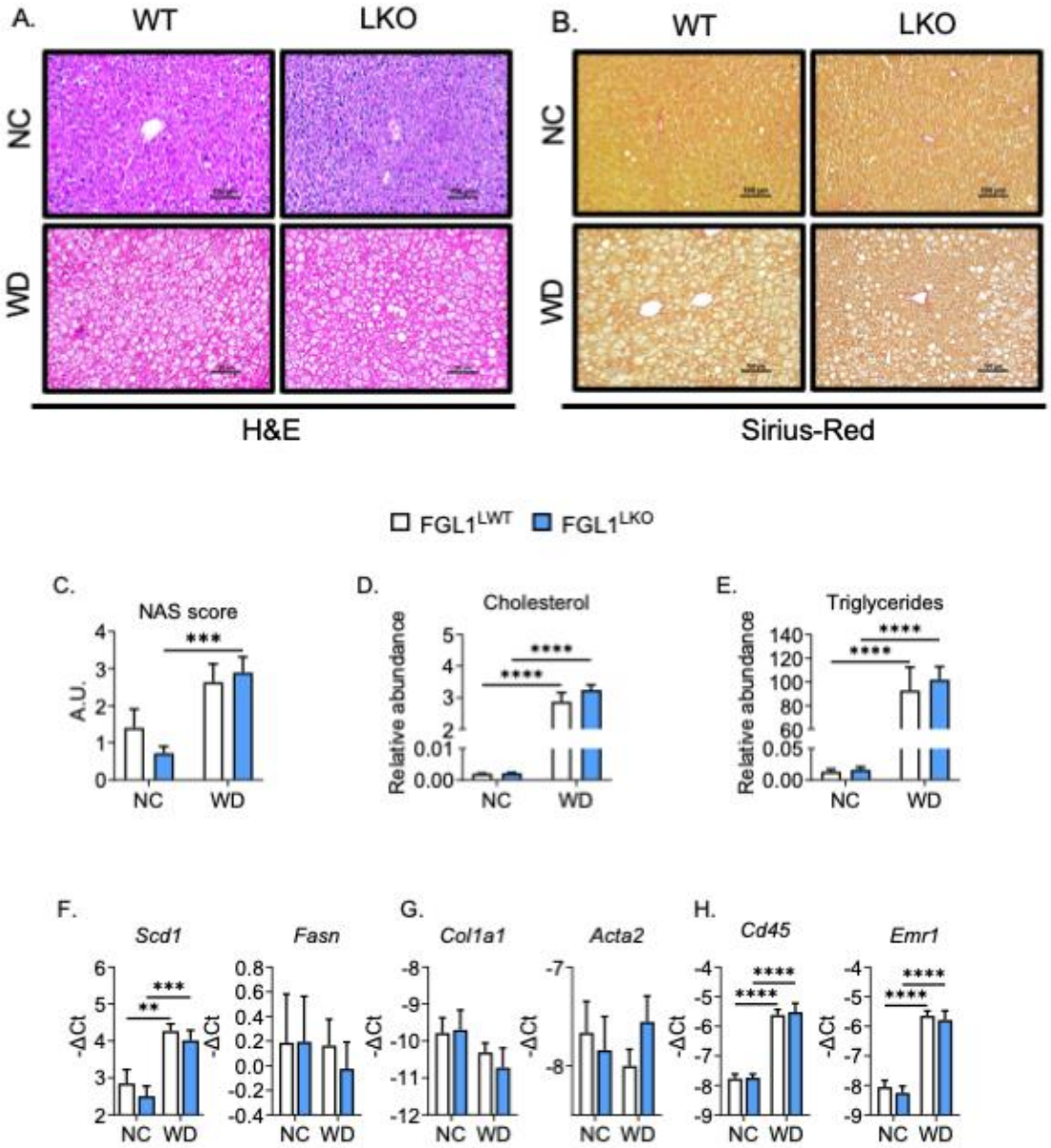

517

518

Figure 4

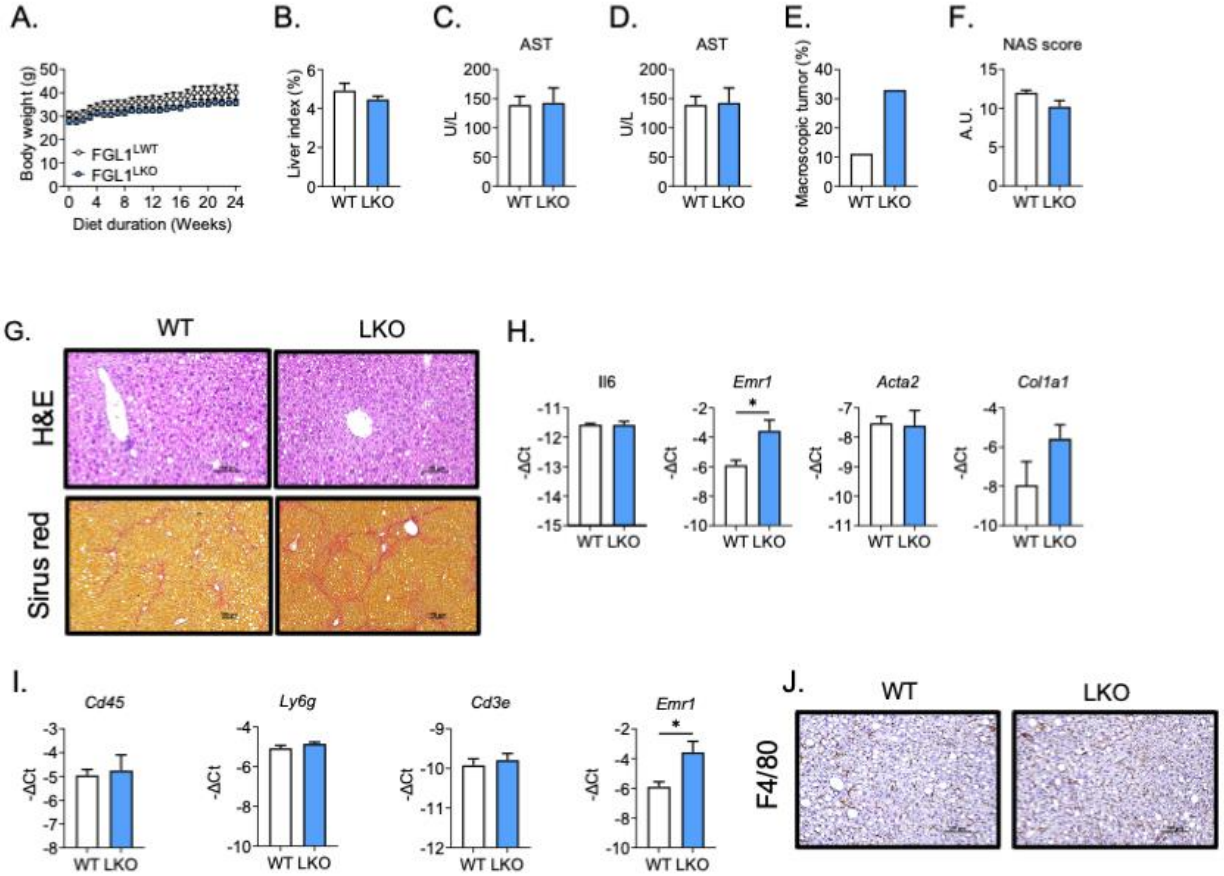
A.
Body weight (g)
FGL1LWT
FGL1LKO
Diet duration (Weeks)
B.
Liver index (%)
WT LKO
C.
AST
U/L
WT LKO
D.
AST
U/L
WT LKO
E.
Macroscopic tumor (%)
WT LKO
F.
NAS score
A.U.
WT LKO
G.
WT
LKO
H&E
Sirus red
H.
Il6
Emr1
Acta2
Col1a1
-ΔCt
WT LKO
I.
Cd45
Ly6g
Cd3e
Emr1
-ΔCt
WT LKO
J.
WT
LKO
F4/80

Figure 5

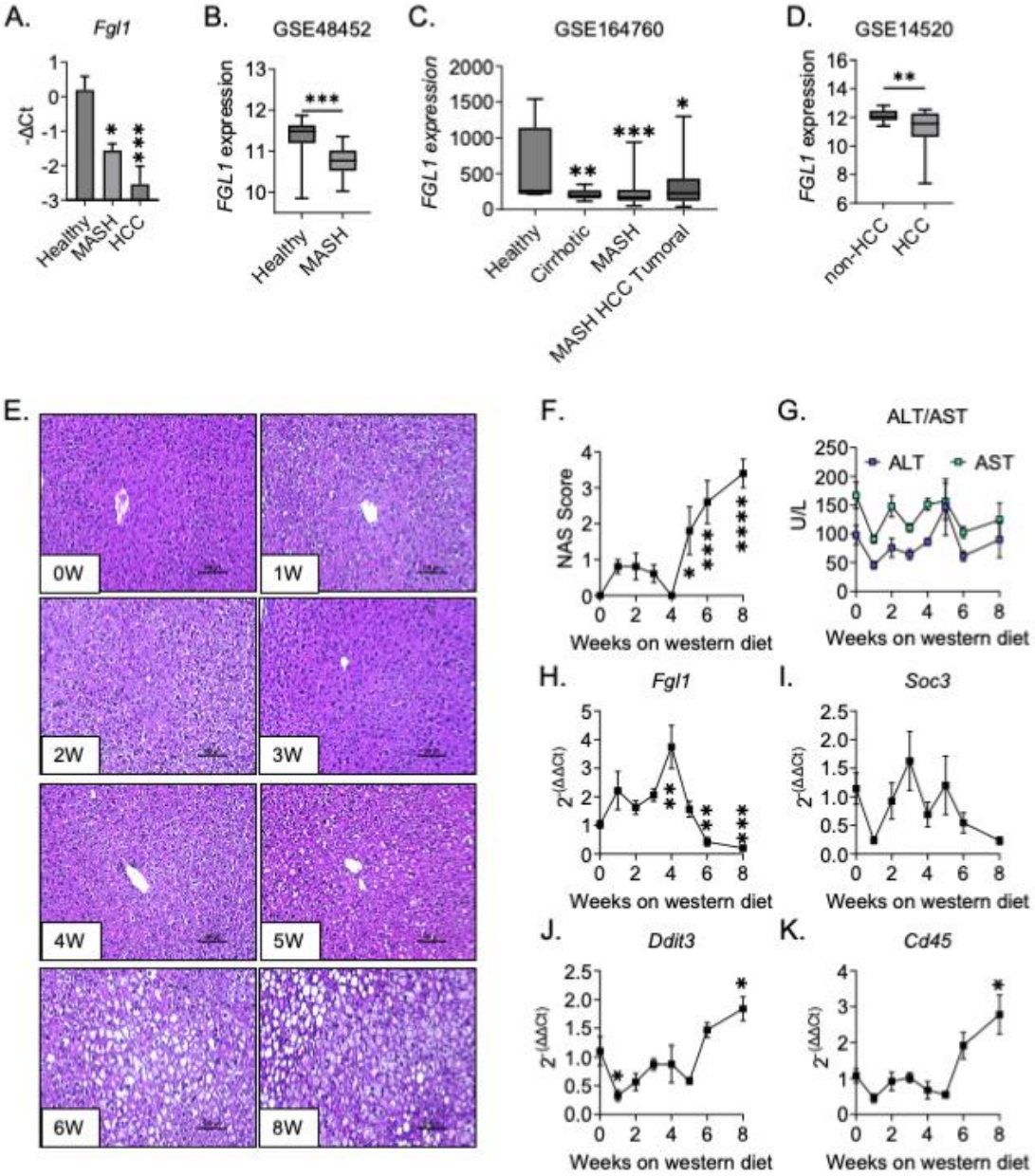
A.
Fgl1
-ΔCt
Healthy
MASH
HCC
B.
GSE48452
FGL1 expression
Healthy
MASH
C.
GSE164760
FGL1 expression
Healthy
Cirrhotic
MASH
MASH HCC Tumoral
D.
GSE14520
FGL1 expression
non-HCC
HCC
E.
0W
1W
2W
3W
4W
5W
6W
8W
F.
NAS Score
Weeks on western diet
G.
ALT/AST
ALT
AST
U/L
Weeks on western diet
H.
Fgl1
Weeks on western diet
I.
Soc3
Weeks on western diet
J.
Ddit3
Weeks on western diet
K.
Cd45
Weeks on western diet

522